Pergamon

PII: S0098-3004(96)00089-1

Computers & Geosciences Vol. 23, No. 3, pp. 283–292, 1997

0098-3004/97 $17.00 + 0.00

SIMULATING LAVA FLOWS BY AN IMPROVED CELLULAR AUTOMATA METHOD

HIDEAKI MIYAMOTO, and SHO SASAKI

Geological Institute, University of Tokyo, Bunkyo-ku, Tokyo, 113, Japan
(*e-mail*: mhideaki@geol.s.u-tokyo.ac.jp)

(Received 9 February 1996; revised 30 August 1996)

Abstract—Lava-flow morphology is determined by cooling rate, viscosity, yield strength, eruption rate, topography, total mass, and other various factors. We have made a numerical flow model, assuming nonisothermal laminar Bingham flow, in which we take the self-gravity and cooling mechanisms into account. Because the calculation method is a type of cellular automata on square meshes, we can apply our numerical model on any actual topography based on a dense-grid digital elevation model. A method of eliminating the mesh shape dependence, which is a well-known problem of cellular automata, is also presented. This reduced random space method enables us to calculate large-scale lava flows in a short time without numerical instability, and obtain mesh-free reliable results. This method is applicable to any other cellular automata type algorithm with ease. We validate our simulation code using data from a real lava flow. © 1997 Elsevier Science Ltd

Key Words: Lava flow, Simulation, Cellular automata, Bingham fluid.

INTRODUCTION

Rheological properties of lava flow, such as viscosity and yield strength, are sometimes measured at terrestrial volcanoes (e.g. Minakami, 1951; Bottinga and Otter, 1971; Murase, McBirney, and Melson, 1985), and often estimated by petrological study (e.g. Shaw, 1969; Murase and McBirney, 1973). Eruption temperatures, gas contents, and flow rates of moving lavas are also measured at some volcanoes (e.g. Pinkerton and Sparks, 1976, 1978; Sparks and Pinkerton, 1978).

However, our understanding of moving lava flows is so limited that even if *in situ* observation and measurements of physical properties of lava are possible it is not yet possible to establish straightforward relationships between properties of lava flows and their morphologies. This difficulty is made worse because the parameters controlling the lava-flow change in space and time, for example when lava flows over complex topography.

Because it is difficult to deal with so many parameters, simplified models have been proposed using approximations (e.g. Wadge, 1978; Huppert, 1982; Huppert and others, 1982; Wilson and Head, 1983; Pieri, 1986; Crisp and Baloga, 1990; Wadge and Lopes, 1991; Dragoni, 1993; Stasiuk, Jaupart, and Sparks, 1993; Bercovici, 1994; Pinkerton and Wilson, 1994). Yet it is difficult to validate such simplified models under general conditions.

Numerical simulation of lava flow is an effective approach because of its potential to deal with many parameters simultaneously and to model topographic features. A number of attempts at numerical simulation of lava flow have been made (e.g. Ishihara, Iguchi, and Kamo, 1990; Young and Wadge, 1990; Wadge and McKendrick, 1993; Barca and others, 1993; Wadge, Young, and McKendrick, 1994). However, most previous works seem to be too simplified: the methods are based on empirically obtained equations for some special lava, and are difficult to apply in general conditions.

Among them, the method of Ishihara (Ishihara, Iguchi, and Kamo, 1990), which is based on the downslope Bingham flow model of Dragoni (Dragoni, Bonafede, and Boschi, 1986) and calculates mass and energy transport, seems to be more realistic than the previously cited works. However, the theory of Dragoni is valid only if the plane is inclined; therefore, it is not possible to calculate the flow on a flat or little inclined plane by Ishihara's method. Also, the model did not consider the flow driven by the pressure gradient as a result of the variation of flow depth across the flow. In this study, we improve Ishihara's method by considering the effect of self-gravity.

The calculation method of Ishihara has another critical weakness: mesh dependence. The mesh shape and direction can cause a bias to the simulation. More than twice the length of lava flow may be produced using the normal cellular automata method than, instead of applying the mesh-free condition. The problem of mesh dependence is an important problem of cellular automata (e.g. Madore and Freedman, 1983). To reduce this problem we

could use a considerably smaller time interval or mesh size. However, this would greatly increase calculation times. We had to eliminate this problem for realistic calculation. To this end, we developed a reduced random space method of cellular automata which can eliminate the mesh bias without increasing calculation time. Using this technique, we developed a more realistic code which can reproduce the morphology of existing small-scale lava flows and has the potential to calculate large-scale lava flows without a numerical instability in a practical time-frame.

THEORY

A fact first proposed by Robson (1967) and now widely accepted is that lava behaves as a Bingham fluid which is characterized by yield strength and plastic viscosity. Here, we consider a lava flow as an incompressible Bingham fluid, which is a good approximation for modeling the macroscopic behavior of simple flows of lava.

Dragoni and co-workers made a simple downslope model of Bingham fluid which is valid only if the plane is inclined (Dragoni, Bonafede, and Boschi, 1986). They did not consider the flow driven by the pressure gradient as a result of the variation of flow depth.

Figure 1 is a cross-section of a simplified lava flow, and we now consider the pressure-driven flow of this model. The x-axis is a direction of flowing lava, α is the inclination of the slope on which lava flows, and β is the angle created by lava thickening. β is an important factor when the slope of the ground, α, is almost zero. We are interested in the situation where the angle α is so small that the vertical flow motion is negligible.

Under these conditions, the Navier–Stokes equation in a steady state is simplified to be a force-balance equation such as:

$$\eta \frac{\partial^2 u}{\partial z^2} = -\frac{\partial h}{\partial x}\rho \mathbf{g} \cos \alpha + \rho \mathbf{g} \sin \alpha, \tag{1}$$

where η is the viscosity, u is the flow velocity, h is the flow thickness, $\mathbf{g}$ is the acceleration as a result of gravity, ρ is the flow density, and α is the angle of the slope. The newly introduced first term of the right-hand side comes from the pressure gradient as a result of the change of lava thickness. For a detailed derivation of Equation (1), see Appendix A. Integrating Equation (1) with $u = 0$ at $z = 0$ as a boundary condition, we obtain

$$\eta \frac{\partial u}{\partial z} = \begin{cases} \rho \mathbf{g}(\sin \alpha - \dfrac{\partial h}{\partial x} \cos \alpha)(h - z) - S_y \\ \quad (\text{for } 0 < z < h - h_c) \\ 0 \\ \quad (\text{for } h - h_c < z < h) \end{cases} \tag{2}$$

where h_c is the critical thickness under which the flow cannot move because the stress is smaller than the yield strength, and S_y is the yield strength which is added by the assumption of Bingham fluid. The critical thickness is expressed as

$$h_c = \frac{S_y}{\rho \mathbf{g} \sin \alpha - \dfrac{\partial h}{\partial x} \rho \mathbf{g} \cos \alpha}. \tag{3}$$

The critical thickness is the thickness of the upper part of the flow, which does not suffer from shear deformation and is often termed a plug. Note that the critical thickness h_c is derived from the assumption of Bingham fluid. In the instance of Newtonian fluid with $S_y = 0$, there is no critical thickness. At the base of the flow, the shear stress has its maximum value, σ,

$$\sigma = \rho \mathbf{g} h (\sin \alpha - \frac{\partial h}{\partial x} \cos \alpha). \tag{4}$$

The lava should stop when the bottom stress is smaller than the yield strength, $\sigma < S_y$, and then the lava thickness becomes smaller than the above-defined critical thickness, $h < h_c$. By integrating Equation (2), the flow velocity below a plug is obtained as

$$u(z) = \frac{1}{\eta}\left[\frac{1}{2}\rho \mathbf{g}(\sin \alpha - \frac{\partial h}{\partial x} \cos \alpha) z(2h - z) - S_y z\right]$$

$$(\text{for } 0 < z < h - h_c). \tag{5}$$

The upper part of lava should flow as a plug as a result of the assumption of Bingham fluid, and its velocity v_p is easily derived from Equations (2) and (5) as

$$v_p = \frac{\sigma h}{2\eta}(1 - \frac{S_y}{\sigma})^2$$

$$(\text{for } z >= h - h_c). \tag{6}$$

Then, the flow rate per unit width is

$$Q = \rho \int_0^h v(z) \mathrm{d}z = \frac{\rho S_y h_c^2}{3\eta}\left[\left(\frac{h}{h_c}\right)^3 - \frac{3}{2}\left(\frac{h}{h_c}\right)^2 + \frac{1}{2}\right]. \tag{7}$$

This fundamental equation is the same as the equation derived by Dragoni (Dragoni, Bonafede, and Boschi, 1986). However, in our formulation, the driving force as a result of changes in flow

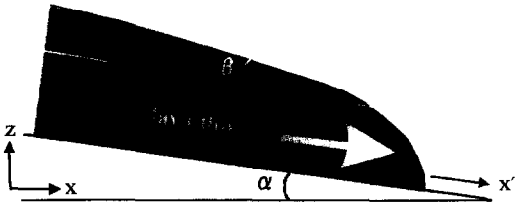

Figure 1. Cross-section of downslope lava flow shown with coordinate system.

depth is taken into account through the expression of h_c [Eq. (3)].

We presume lava to be an incompressible fluid with the equation of continuity as

$$\mathrm{div}(\rho u) = 0. \tag{8}$$

The equation for heat loss is given by

$$\rho C_p \frac{\partial T}{\partial t} = -\epsilon \sigma_{SB} T^4, \tag{9}$$

where C_p is the specific heat, ϵ is the emissivity and σ_{SB} is the Stefan–Boltzmann constant ($=5.67 \times 10^{-8}$W m^{-2} K^{-4}). In Equation (9), we take into account only the most important process (radiation heat loss), and we neglect heat conduction to the atmosphere and to the ground, vertical temperature variation, and viscous dissipation.

METHOD

To calculate the flow rate with Equation (7), some parameters should be known. Although we can consider ρ and g as constants, S_y, η, $\partial h/\partial x$, h, and α may change in time and space.

Our method of calculation is similar to that of Ishihara (Ishihara, Iguchi, and Kamo, 1990), and is illustrated in Figure 2. Before computation, the calculation area should be divided into a mesh with square cells. Each cell has values of altitude and lava thickness. The value of altitude represents the average of the actual topography in the cell. The net volume of lava in each cell is equal to the product of the area and the lava-flow thickness of the cell. Each cell also has an average lava temperature, so the heat of the lava in the mesh is equal to the product of the volume and the average temperature.

The volume is changed by lava eruption or mass transport of lava. The eruption from the vent is represented by the increasing volume of lava at the corresponding cells. The product of the vent area and lava thickening rate is the eruption rate. The lava does not move when the thickness is below its critical thickness. If the thickness attains the critical thickness, outflows, or mass transports, to the adjacent cells occur, and they enhance the thicknesses of adjacent cells.

The flow rate is calculated by Equation (7). Now we consider a flow from the cell (i, j) to the cell $(i + 1, j)$ for example. The increase in volume of the cell $(i + 1, j)$ as a result of the flow from the cell (i, j) during a time interval Δt is

$$\Delta V = \frac{\rho S_y h_c^2 w}{3\eta}\left[\left(\frac{h}{h_c}\right)^3 - \frac{3}{2}\left(\frac{h}{h_c}\right)^2 + \frac{1}{2}\right]\Delta t, \tag{10}$$

where V is the lava volume of the cell $(i + 1, j)$ and w is the width of cell. The yield strength and the viscosity for the cell (i, j) are used for S_y and η in Equation (10). The critical thickness h_c in Equation (10) is calculated by Equation (3) using an approximation, $\partial h/\partial x \approx \Delta h/w$, where Δh is thickness difference between the cell (i, j) and the cell $(i + 1, j)$.

The heat is transferred in accordance with the mass transport. Temperature change as a result of radiative heat loss from the surface is also involved. The viscosity and yield strength are calculated from the temperature at the cell. The calculation advances until no further flow is possible.

SOLUTION OF THE ANISOTROPIC PROBLEM

The cellular automata method has a well-known problem of mesh dependence (e.g. Markus and Hess, 1990). Here we show a solution to this problem without increasing the calculation time. Consider a lava that erupts on a flat plane. Although the lava should spread axisymmetrically under its own hydrostatic pressure and form a lava dome, numerical results of previous cellular automata methods on a plane are affected by the square shape of meshes (Fig. 3). The calculated length of lava flow depends on the relative directions of flow

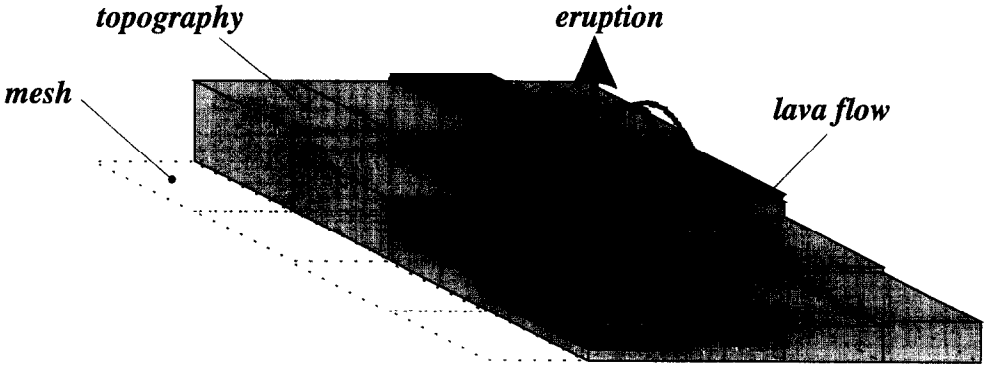

Figure 2. Sketch of numerical method of lava flow. Parallelograms shown by dotted line represent meshes, lightly shaded rectangular boxes and darkly shaded rectangular boxes represent topographies and lava flows, respectively. Lava erupts and flows downwards because of ground inclination and gravity.

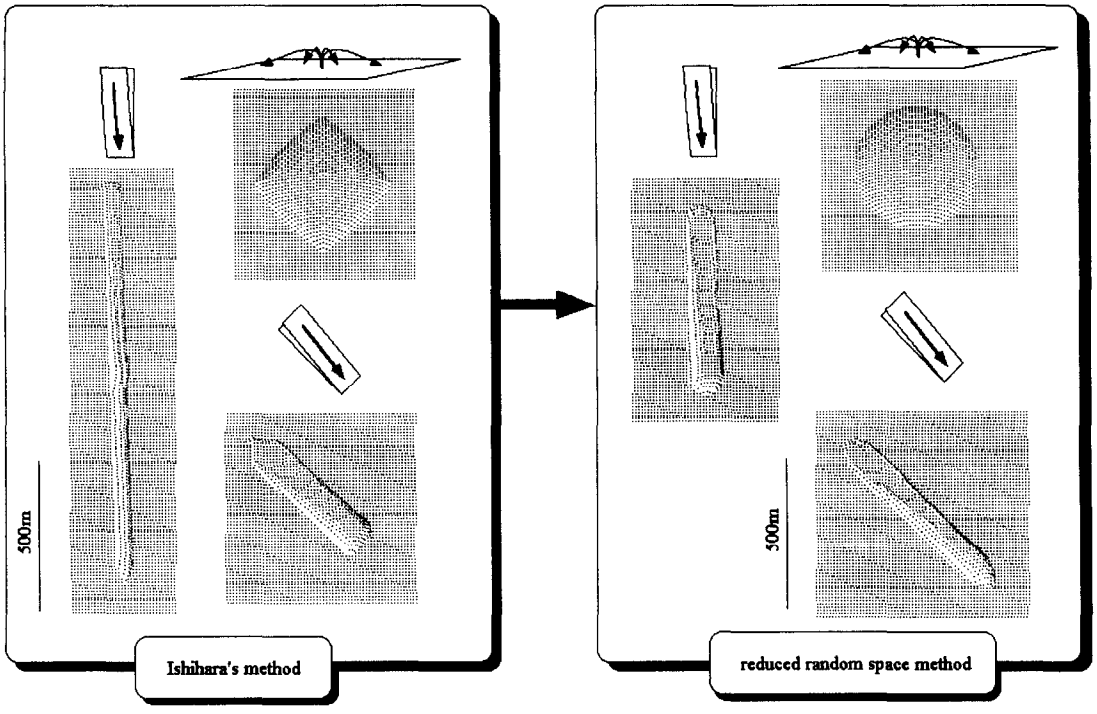

Figure 3. Results of Ishihara's method with our newly introduced equations (left), and this work (right) with same conditions for basalt type lava flow. Each group consists of three calculations: eruption on flat plane (right-upper figure in each group), eruption on slope with inclination angle 5° (left- and right-lower figure in each group). Note that two figures in each group are results on same inclination, but directions of inclination are different; lengths of these results should be same. On flat plane, lava should spread axisymmetrically. Whereas mesh dependencies clearly appear in previous results, results of this work have no dependence on mesh direction.

and the mesh: the length of lava which goes down one of the principal directions of the mesh is about 1.3 times longer than that in the diagonal direction. The error from this discrepancy is significant in large-scale lava-flow simulations.

We developed a program based on hexagonal meshes to resolve this problem, and we simply obtained a hexagonal feature where flow moves faster along the mesh direction.

The reason why this problem occurs is that the flux between adjacent cells is not linearly proportional to the thickness of lava in our lava-flow model. For sufficiently thin thicknesses the flow calculated by Equation (7) can be regarded as linear. This condition requires a extremely small time interval, and an unrealistically long simulation time. Accordingly, we must look for another strategy for efficient calculation.

Here we consider a cellular automaton which has randomized representative points. Figure 4 shows the mesh geometry. One point is placed randomly in each cell. This point represents the entire area of the cell that includes the point. Because only flows to the adjacent cells are considered in our method, the exact relationship between adjacent cells is important for such randomly given points. We now define a neighborhood by a circle with an arbitrary radius R on a given point. Every point in this circle is within the neighborhood. With constant value of R we can determine the probability of whether the point of each cell is in the neighborhood. The flows to adjacent cells can be distributed based on this probability. If we use a large value of R to include many points we may have more accurate results, but the calculation time will increase with R^2.

Here, we suppose that the width of each cell is sufficient for the value of R. Then we should know average probabilities of whether the representative

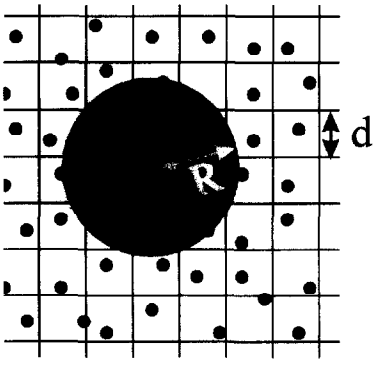

Figure 4. Cell geometry of cellular automaton with randomized representative points. d is grid spacing. Every point in shaded circle whose radius is R is within neighborhood.

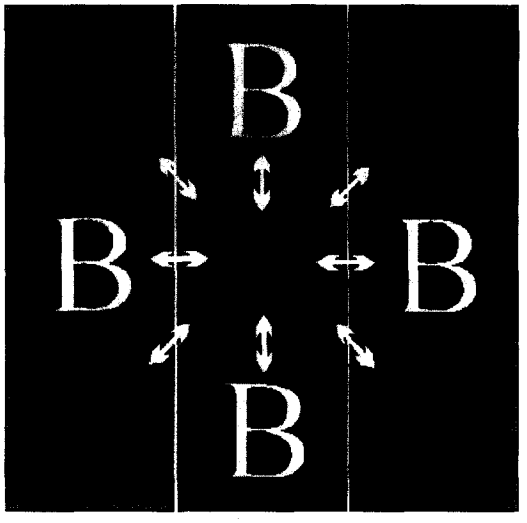

Figure 5. Mesh with central point is shown as C area. Adjacent meshes are divided into two regions, A and B. Probability for A and B regions can be estimated analytically, see text.

point of each cell is involved in the circle, where R is the width of cell. As shown in Figure 5, eight cells are adjacent and they are of two types: A and B. The probability for regions A and B can be estimated analytically. If the point of the central cell is provided, the "overlapping area" between a target cell and the circle is proportional to the probability of whether the point in the cell is enclosed by the circle.

Let the coordinates of the central point be (a, b) as shown in Figure 6. The overlapping area is calculated as

$$\int_{x=-\sqrt{d^2-b^2}+a}^{0} \sqrt{d^2-(x-a)^2}-b\,\mathrm{d}x, \qquad (11)$$

where d is the width of the cell, and is equal to the radius of the circle, R.

The average of the overlapping area of the target cell and every circle whose center is in the central cell is proportional to the probability of the target cell.

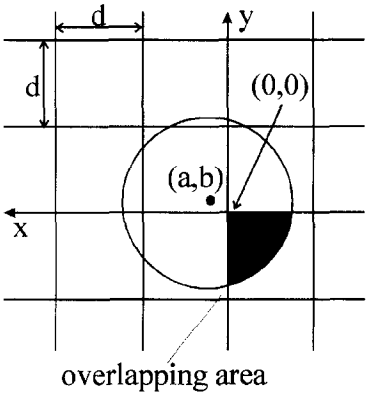

Figure 6. Coordinate systems for analytical estimation of probability. Overlapping area between target cell and circle is proportional to probability of whether randomly given point in cell is enclosed by circle, see text.

From Equation (11), the average of overlapping area for A region, P_A, is expressed as

$$P_A = \frac{1}{d^2}\int_{b=0}^{d}\int_{a=0}^{\sqrt{d^2-b^2}}\int_{x=-\sqrt{d^2-b^2}+a}^{0}\sqrt{d^2-(x-a)^2} - b\,\mathrm{d}x\,\mathrm{d}a\,\mathrm{d}b \qquad (12)$$

and is equal to $1/8d^2$.

The sum for B region P_B is

$$P_B = \frac{1}{d^2}\int_{b=0}^{d}\int_{a=0}^{d}\int_{x=-\sqrt{d^2-b^2}+a}^{\sqrt{d^2-b^2}+a}\sqrt{d^2-(x-a)^2} - b\,\mathrm{d}x\,\mathrm{d}a\,\mathrm{d}b - 2\times P_A, \qquad (13)$$

and is equal to $5/12d^2$.

The area of B region is 10/3 times larger than that of A region. This implies that we should calculate flow to A region three times, whereas we calculate flow to B region ten times.

In our program, we use random numbers generated by the computer. After calculation of flow to A region, a random number is obtained. This random number takes a value from zero to one. When the number is greater than 0.7, we calculate the flow to B region, otherwise we do not calculate the flow.

Under this approximation, which we term a reduced random space cellular automaton, we have no dependence of the direction of the mesh as shown in Figure 3. This justifies using equal values of R as the cell width.

PROGRAM DESCRIPTION

Figure 7 depicts a flowchart of the main operations of the program. Listings of C programs, a Makefile, and some header files are publicly available by anonymous FTP from the server IAMG.ORG, or from http://www.iamg.org.

The following input data and parameters are required by the program:

(1) digital topography data (digital elevation model, DEM);
(2) positions of vents;
(3) extrusion rate and temperature;
(4) duration of extrusion;
(5) time interval and duration of calculation;
(6) density, emissivity and specific heat of lava;
(7) ground temperature;
(8) tables of viscosity and yield strength versus temperature.

The DEM width, height, and parameters (2)–(8) should be given to the program as a header file, "constants.h" (see Appendix B). In operation the program follows the sequence of calculations:

(1) Initialize all cells; lava thickness and lava temperature are all set to zero. The table of vis-

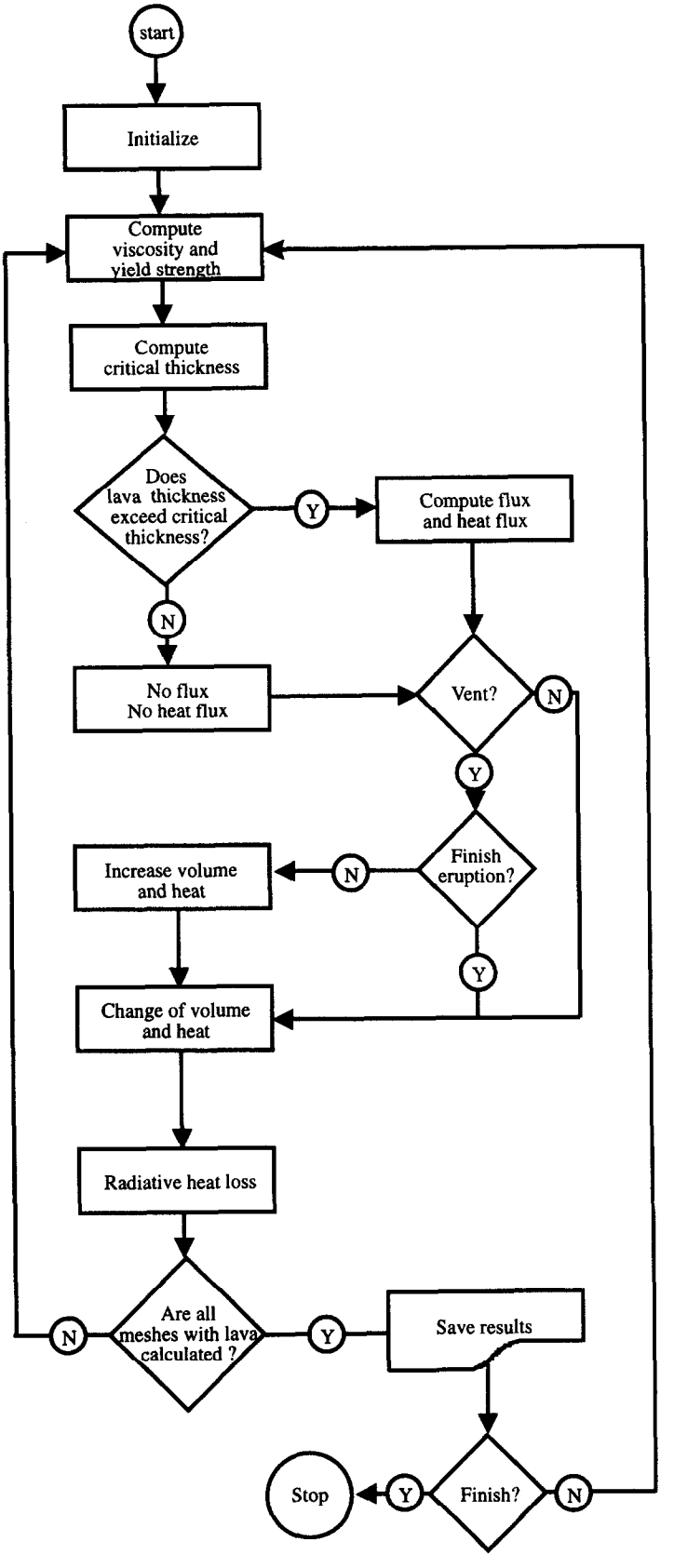

Figure 7. Flowchart of our method.

cosity and yield strength are calculated and saved in memory.

(2) Calculate viscosity, yield strength, and critical thickness.

(3) If the lava thickness is larger than the critical thickness, calculate flux between two adjacent cells.

(4) Steps 2 and 3 are repeated for four adjacent cells (B region in Fig. 5) and four diagonal cells (A region) with the reduced random space method.

(5) Steps 2–4 are repeated for every cell which has lava.

(6) Increase volume of lava at vent cells according to lava eruption rate.

(7) Calculate heat flux between adjacent cells, and cooling by radiation. Then calculate temperature from heat exchange.

(8) Continue calculation within the given calculation time.

Each cell of our method has four data values: the x-coordinate, the y-coordinate, the lava thickness, and temperature. Hence, outputs of our program consist of the thickness data files and the temperature data files. Thickness and temperature values are written as a one-dimensional data set. For example, the contents of a 3×3 thickness data file is ordered as: (1,1), (2,1), (3,1), (1,2),..., (2,3), (3,3). The thickness and temperature data files are produced in a certain time-interval, giving multiple pairs of data files at the end of each simulation.

RESULTS

To check the validity of our method we computed an isothermal two-dimensional flow, there being no analytical study of nonisothermal Bingham flow. We calculated two-dimensional isothermal flow with a Bingham assumption on a flat plane to compare with the morphology of the analytical theory developed by Hulme (1974).

We have calculated two-dimensional symmetric flow away from a central vent. We assume isothermal lava where viscosity and yield strength are constant throughout the flow. The outline of a typical flow is shown in Figure 8, and parameters for this are listed in Table 1. Eruption ceased at $t = 1000$ sec. Then the lava thickness gradually becomes thinner.

In Hulme's (Hulme, 1974) analytical solution the flow on a horizontal plane is driven by the pressure gradient as a result of the variation of flow depth across the flow, and the flow stops when shear stress at the bottom becomes less than the yield strength of lava. The transverse profile of the flow is expressed as

$$h^2 = \frac{2S_y}{\mathbf{g}\rho}\left(\frac{w}{2} - x\right), \tag{14}$$

where h is the thickness of lava flow at a distance x from the center of the flow, and w is the width of the flow. From this equation, we can see that the outline of the Bingham fluid on a flat plane should be a pair of parabolic curves. Our results are consistent with this prediction. The maximum flow depth is attained at the center of the flow. From Equation (14), by putting $x = 0$, the maximum flow depth, h_0, is

$$h_0^2 = \frac{S_y w}{\mathbf{g}\rho}. \tag{15}$$

This is a theoretical equation of the relationship between flow height and flow width at steady state.

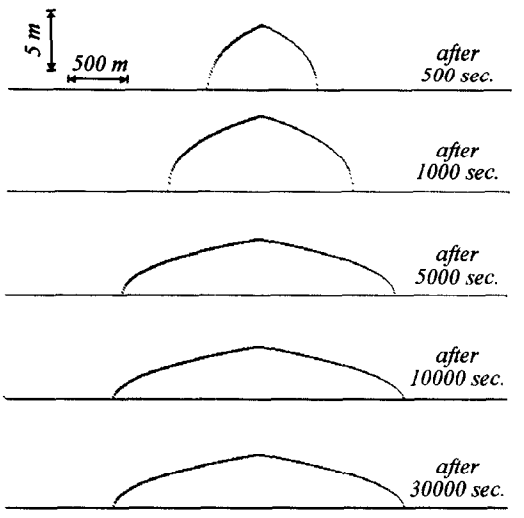

Figure 8. Outline of typical two-dimensional flow. Note that outline consists of pair of parabolic curves resulting from effect of yield strength.

The differences between numerically obtained values and theoretical values of lava thickness are shown in Figure 9. The width, thickness, and difference of calculated and theoretical thickness (error) of the flow are given as functions of time. The thickness and width do not change after $t = 25{,}000$ sec, and then we obtain a good agreement between theoretical and calculated values, which is reasonable because the theory of Hulme is valid only in the steady state. These results confirm the validity of our method of two-dimensional flow.

Table 1. Simulation parameters for typical two-dimensional flow

Parameter	Value
Specific heat	840 J kg^{-1} K^{-1}
Eruption rate	100 m^3 sec^{-1}
Emissivity	0.9
Viscosity	850 Pa sec^{-1}
Yield strength	225 N m^{-2}
Eruption duration	1000 sec
Density	2500 kg m^{-3}
Gravity	9.8 m s^{-2}
Cell width	10 m

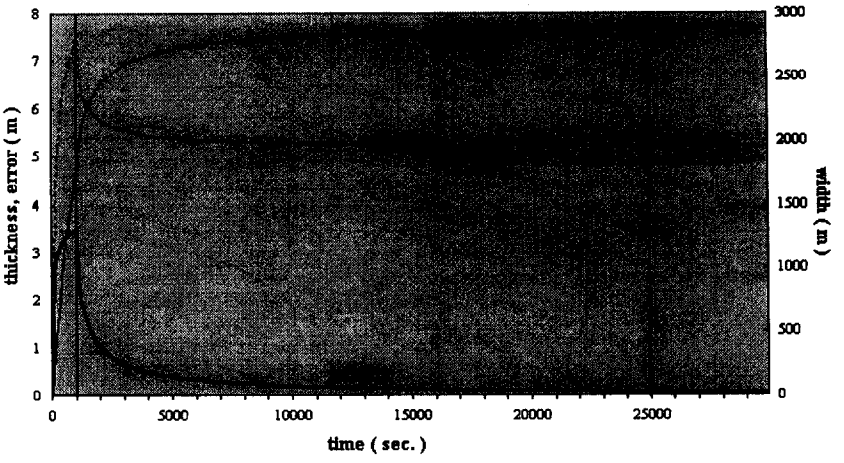

Figure 9. Difference between numerically obtained values and theoretical values of lava thickness, showing good agreement.

We also used our model to simulate actual lava flows. To perform this simulation, we have to assume some parameters, such as the location of the vents, eruption rate, eruption duration, relations between viscosity and temperature, relations between yield strength and temperature, and topographic data before eruption.

The 1983 Miyakejima lava flow (34°05′N, 139°32′E) is good for our purpose because topographic data prior to the eruption are available, the physical properties of the lava were investigated, and the advance of the flowing lava was observed (Aramaki and Hayakawa, 1984; Soya, Uto, and Suto, 1984; Fujii and others, 1984). We used field observations for viscosity and yield strength, and assumed the values of eruption rate and the location of the vent.

Figure 10 is the result of the simulation using the parameters shown in Table 2. The result shows a similar morphology as the actual lava flow, although there are some differences from the actual flow. Most differences appear around the vent, so it seems that either the estimation of eruption rate or the location of the vent is different from the actual eruption. The rate of advance of the simulated flow agrees well with the observed flow advance.

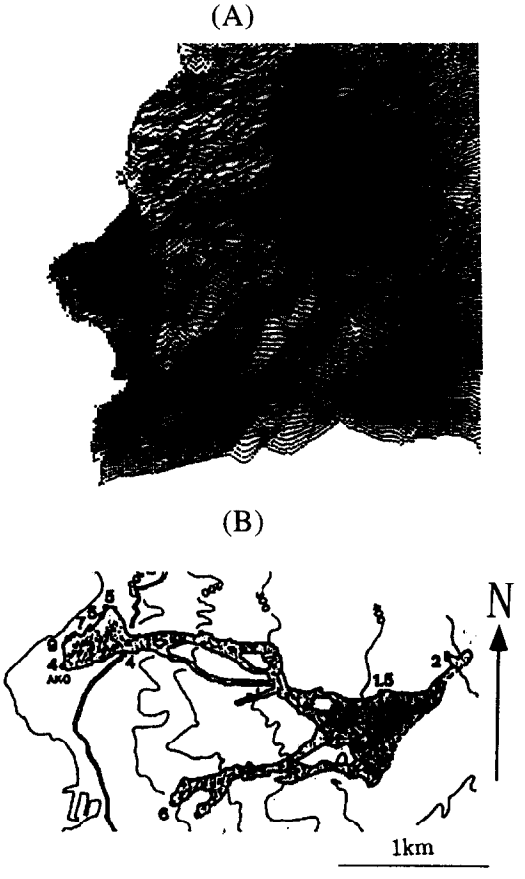

Figure 10. Simulation result of 1983 Miyakejima lava flow (A) in comparison with actual flow (B). Good agreement in morphology, except for differences around vents, because of estimation of eruption rate or vent location.

CONCLUSION

An improved cellular automata method of lava flow based on the theory of steady-state Bingham

Table 2. Simulation parameters for 1983 Miyakejima lava flow

Parameter	Value
Specific heat	840 J $kg^{-1}K^{-1}$
Eruption rate	130 m^3 sec^{-1}
Emissivity	0.9
Eruption viscosity	850 Pa sec^{-1}
Eruption yield strength	225 N m^{-2}
Eruption temperature	1320 K
Eruption duration	7200 sec
Density	2500 kg m^{-3}
Gravity	9.8 m sec^{-2}
Atmospheric temperature	300 K
Cell width	10 m

flow has been developed. With the limitations of two-dimensional and isothermal conditions which is added to check the validity, the calculated results agree well with the theoretical relationship between lava thickness and width. Our method eliminated the dependence on the direction of the mesh, so we can calculate lava-flow morphology easily, accurately and effectively. The good agreement of simulated and the actual lava flow at Miyakejima in 1983 adds to the validity of our method, and also may enable the physical properties of existing lava flows to be identified.

Acknowledgments –We would like to thank Dr N. Nishiwaki of Nara University, Japan, and Dr D. F. Merriam of the Kansas Geological Survey for their encouragement at the IAMG '95 conference, where this paper was presented. We thank the anonymous reviewers whose comments improved the original manuscript.

REFERENCES

Aramaki, S., and Hayakawa, Y., 1984, Sequence and mode of eruption of the October 3–4, 1983 eruption of Miyakejima: Bull. Volcanol. Soc. Japan, v. 29, p. S24–S35 (special issue on the 1983 eruption of Miyakejima, in Japanese).

Barca, D., Crisci, G. M., Di Gregorio, S., and Nicoletta, F., 1993, Cellular automata methods for modelling lava flows: simulation of the 1986 1987 eruption, mount Etna, Sicilly, *in* Kilburn, C. R. J. and Luongo, G. eds., Active Lavas: Monitoring and Modelling: UCL Press, London, p. 374.

Bercovici, D., 1994, A theoretical model of cooling viscous gravity currents with temperature-dependent viscosity: Geophys. Res. Lett., v. 21, no. 12, p. 1177–1180.

Bottinga, Y., and Otter, J. L., 1971, The viscosity of silicate magmatic liquids: Am. Jour. Sci., v. 272, p. 438–475.

Crisp, J., and Baloga, S., 1990, A model for lava flows with two thermal components: Jour. Geophys. Res., v. 95, p. 1255–1270.

Dragoni, M., 1993, Modelling the rheology and cooling of lava flows, *in* Kilburn, C. R. J. and Luongo, G., eds., Active Lavas: Monitoring and Modelling: UCL Press, London, p. 374.

Dragoni, M., Bonafede, M., and Boschi, E., 1986, Downslope flow models of a Bingham liquid: implications for lava flows: Jour. Volcanology Geotherm. Res., v. 30, p. 305–325.

Fujii, T., Aramaki, S., Fukuoka, T., and Chiba, T., 1984, Petrology of the ejecta and lavas of the 1983 eruption of Miyakejima: Bull. Volcanology Soc. Japan, v. 29, p. S266–S282 (special issue on the 1983 eruption of Miyakejima, in Japanese).

Hulme, G., 1974, The interpretation of lava flow morphology: Geophys. Jour. Roy. Astronomical Soc., v. 39, p. 361–383.

Huppert, H. E., 1982, Flow and instability of a viscous current down a slope: Nature, v. 300, p. 427–429.

Huppert, H. E., Shepherd, J. B., Sigurdsson, H., and Sparks, R. S. J., 1982, On lava dome growth, with reference to the 1979 extrusion of the Soufriere of St Vincent: Jour. Volcanology Geotherm. Res., v. 14, p. 199–222.

Ishihara, K., Iguchi, M., and Kamo, K., 1990, Numerical simulation of lava flows on some volcanoes in Japan, *in* Fink, J.H., Lava Flows and Domes: Emplacement Mechanisms and Hazard Implications: Springer, Berlin, p. 174–207.

Madore, B. F., and Freedman, W. L., 1983, Computer simulations of the Belousov–Zhabotinsky reaction: Science, v. 222, p. 615–616.

Markus, M., and Hess, B., 1990, Isotropic cellular automaton for modelling excitable media: Nature, v. 347, p. 56–58.

Minakami, T., 1951, On the temperature and viscosity of the fresh lava extruded in the 1951 Oo-sima eruption (in Japanese): Bull. Earthquake Res., v. 24, p. 161–169.

Murase, T., and McBirney, A. R., 1973, Properties of some common igneous rocks and their melts at high temperatures: Geol. Soc. Am. Bull., v. 84, p. 3563–3592.

Murase, T., McBirney, A. R., and Melson, W. G., 1985, Viscosity of the dome of Mount St Helens: Jour. Volcanology Geotherm. Res., v. 24, p. 193–204.

Pieri, D. C., 1986, Eruption rate, area, and length relationship for some Hawaiian lava flows: Jour. Volcanology Geotherm. Res., v. 30, p. 29–45.

Pinkerton, H., and Sparks, R. S. J., 1976, The 1975 subterminal lavas, Mount Etna: a case history of the formation of a compound lava field: Jour. Volcanology Geotherm. Res., v. 1, p. 167–182.

Pinkerton, H., and Sparks, R. S. J., 1978, Field measurements of the rheology of lava: Nature, v. 276, p. 383–385.

Pinkerton, H., and Wilson, L., 1994, Factors controlling the lengths of channel-fed lava flows: Bull. Volcanology, v. 56, p. 108–120.

Robson, G. R., 1967, Thickness of Etnean lavas: Nature, v. 216, p. 251–252.

Shaw, H. R., 1969, Rheology of basalt in the melting range: Jour. Petrology, v. 10, p. 510–534.

Soya, T., Uto, K., and Suto, S., 1984, The products of the 1983 eruption of the Miyakejima Volcano—with special reference to the lava: Bull. Volcanology Soc. Japan, v. 29, p. S230–S241 (special issue on the 1983 eruption of Miyakejima, in Japanese).

Sparks, R. S. J., and Pinkerton, H., 1978, Effect of degassing on rheology of basaltic lava: Nature, v. 276, p. 385–386.

Stasiuk, M. V., Jaupart, C., and Sparks, R. S. J., 1993, Influence of cooling on lava-flow dynamics: Geology, v. 21, p. 335–338.

Wadge, G., 1978, Effusion rate and the shape of a lava flow fields on Mount Etna: Geology, v. 6, p. 503–506.

Wadge, G., and Lopes, R. M. C., 1991, The lobes of lava flows on Earth and Olympus mons Mars: Bull. Volcanology, v. 54, p. 10–24.

Wadge, G. and McKendrick, I., 1993, Computer simulation and zonation of lava flow hazards: in Proc. IDNDR Conf., Royal Society, London, p. 283–291.

Wadge, G., Young, P. A. V., and McKendrick, I. J., 1994, Mapping flow hazards using computer simulation: Jour. Geophys. Res., v. 99, p. 489–504.

Wilson, L., and Head, J. W., 1983, A comparison of volcanic eruption processes on Earth, Moon, Mars, Io and Venus: Nature, v. 302, p. 663–669.

Young, P., and Wadge, G., 1990, FLOWFRONT: simulation of a lava flow: Computers & Geosciences, v. 16, no. 8, p. 1171–1191.

APPENDIX A

Here, we will show the derivation of Equation (1). We start from the Navier–Stokes equation:

$$\frac{Du}{Dt} = K - \frac{1}{\rho}\operatorname{grad} p + \frac{\eta}{\rho}\Delta u,$$

where u is the flow velocity, K is the external force, ρ is the flow density, p is the pressure, and η is the viscosity.

We consider sufficiently slow-moving flow, which is termed the Stokes approximation. With the assumption of steady-state flow, we obtain

$$\eta \frac{\partial^2 u}{\partial z^2} - \text{grad}\, p^* = 0, \quad p^* = p + \rho\Omega$$

where v (u, v) is velocity, and Ω is the external preservative force.

The force balance in the fluid is expressed as

$$\text{grad}\, p^* = \rho \mathbf{g} \tan(\alpha + \beta) \cos\alpha,$$

where $\mathbf{g}$ is acceleration as a result of gravity. If α is sufficiently small, the above is reduced to

$$\text{grad}\, p^* = \rho \mathbf{g} (\sin\alpha - \cos\alpha \tan\beta)$$

With a further approximation, such as

$$\tan\beta \approx \frac{\partial h'}{\partial x'} \approx \frac{\partial h}{\partial x},$$

where x' is the axis parallel to the direction of lava, h is the actual thickness of lava, and h' is the length of the perpendicular from a lava surface to the x' axis (see Fig. 1). We can then obtain Equation (1) of the text:

$$\eta \frac{\partial^2 u}{\partial z^2} = -\frac{\partial h}{\partial x} \rho \mathbf{g} \cos\alpha + \rho \mathbf{g} \sin\alpha$$

APPENDIX B

```
/*******************************************************
        constants.h    ( lf )
 Configure this file to change calculation conditions.
*******************************************************/
#define Max_width  100       /* DEM width */
#define Max_height 100       /* DEM height */
#define fntime     300000    /* end of calculation */
#define e_time     100000    /* end of erruption of all craters */
#define d_time_orig     0.1  /* delta t */
#define d_time_after_errupt 1 /* delta t after e_after_time */
#define e_after_time 100000
#define density    2500.0    /* lava density */
#define gravity    9.8
#define cell_width 10.0      /* mesh size */
#define file_name  "out"     /* file name for output */
#define in_file_name "in"    /* file name for DEM */
#define float double
#define hcapacity  840.0     /* heat capacity of lava */
#define emissivity 1.0       /* emissivity of lava */
#define sbconstant 0.000000058 /* Stefan-Borlzmann constant */
#define ground_tmp 300       /* ground temperature (K) */
#define extrude_x  50        /* vent position */
#define extrude_y  20
#define extrude_to_x 1       /* vent width */
#define extrude_to_y 1
#define extrude    0.1       /* *width*width=extrude rate */
#define t_extrude  1350      /* extrude temperature */
#define  vis_table  pow(10,(20.000*(exp(-0.001835*(i-273)))))
     /* calculate viscosity (Pa.s)  i = temperature */
#define  yie_table  pow(10,(11.67-0.0089*(i-273)))
     /* calculate yield strength ( N/m^2 ) i = temperature */
```